Supplementary information

All-fibrous, permeable, adhesive, and stretchable self-powered electronic skin for sign language recognition

Fan Chen,‡[a] Xian Song,‡[a,e] Jingjing Fu,[a] Jiaheng Liang,[a] Junhua Zhou,[a] Jiehua Cai,[a] Yufei Zhang,[b] Mengjia Zhu,[f] Yichun Ding,[b,f] Jinxing Jiang,[b] Zijian Chen,[b] Youchao Qi,[b] Zhihao Zhou,[a] Qiyao Huang,[b,c] Yingying Zhang,[f] and Zijian Zheng*[a,b,c,d]

[a.] Department of Applied Biology and Chemical Technology, The Hong Kong Polytechnic University, Hong Kong SAR, China.

[b.] School of Fashion and Textiles, The Hong Kong Polytechnic University, Hong Kong SAR, China.

[c.] Research Institute for Intelligent Wearable Systems (RI-IWEAR), The Hong Kong Polytechnic University, Hong Kong SAR, China.

[d.] Research Institute for Smart Energy (RISE), The Hong Kong Polytechnic University, Hong Kong SAR, China.

[e.] Department of Sports Science, Zhejiang University, Hangzhou, China.

[f.] Department of Chemistry, Tsinghua Unviersity, Beijing, China.

‡ These authors contributed equally to this work.

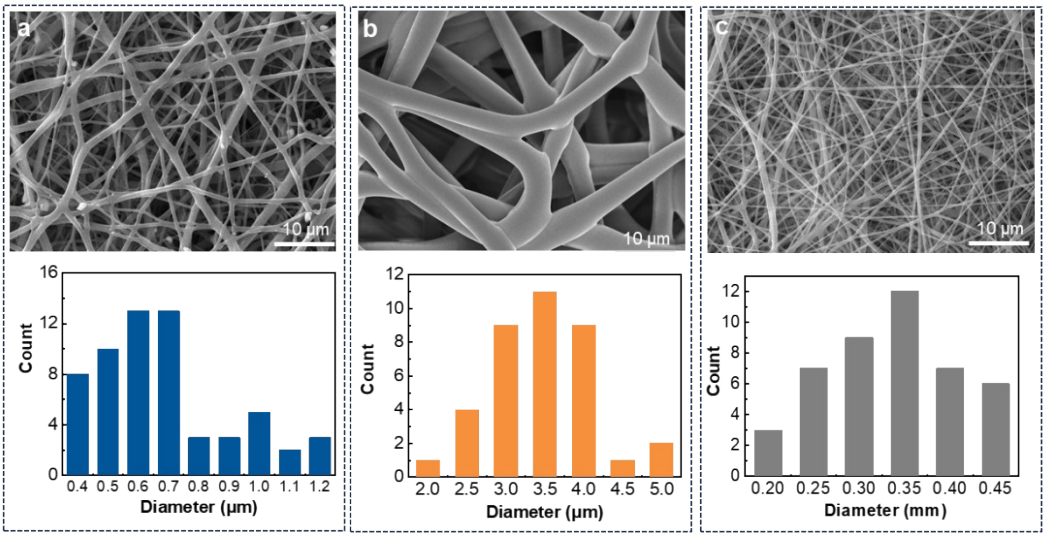

Supplementary Figure 1. a-c, SEM images and diameter distributions of TPU@P(VDF-TrFE) core-sheath fiber mat (**a**), TPU fiber mat (**b**), and adhesive PAAND fiber mat (**c**).

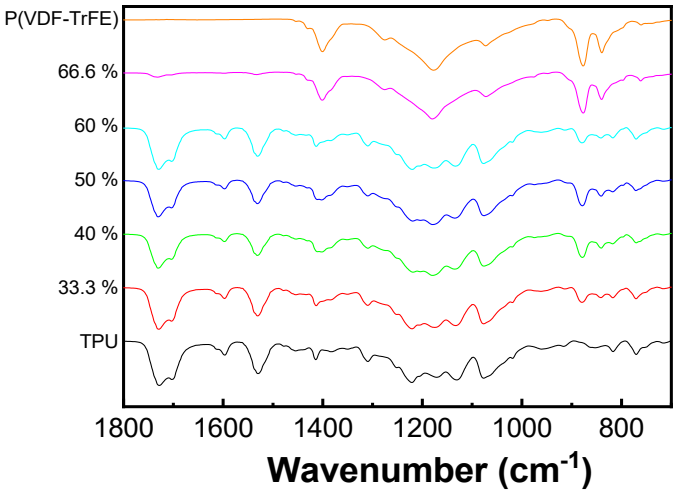

Supplementary Figure 2. Fourier transform infrared spectroscopy (FT-IR) spectrums of TPU, P(VDF), and TPU@P(VDF-TrFE) core-sheath fiber mats.

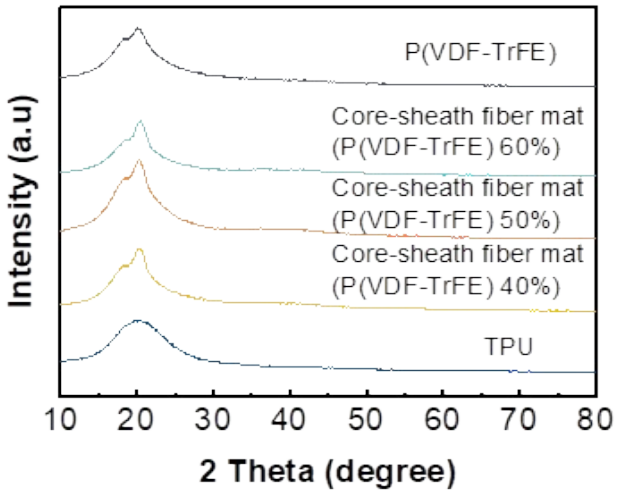

Supplementary Figure 3. X-Ray diffraction (XRD) patterns of TPU, P(VDF), and TPU@P(VDF-TrFE) core-sheath fiber mats.

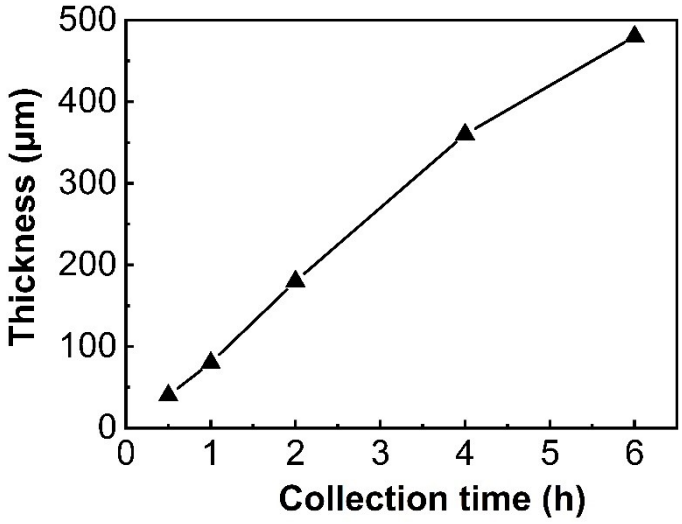

Supplementary Figure 4. Effect of collection time during electrospinning on the thickness for TPU@P(VDF-TrFE) core-sheath fiber mats.

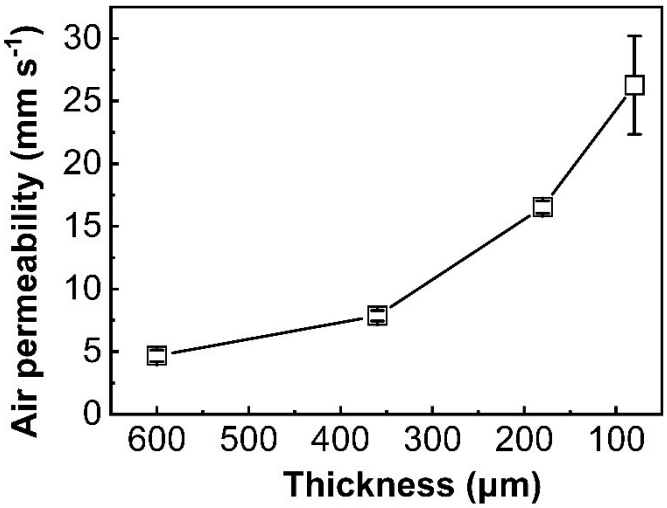

Supplementary Figure 5. Air permeability of core-sheath TPU@P(VDF-TrFE) fiber mat with varying thicknesses.

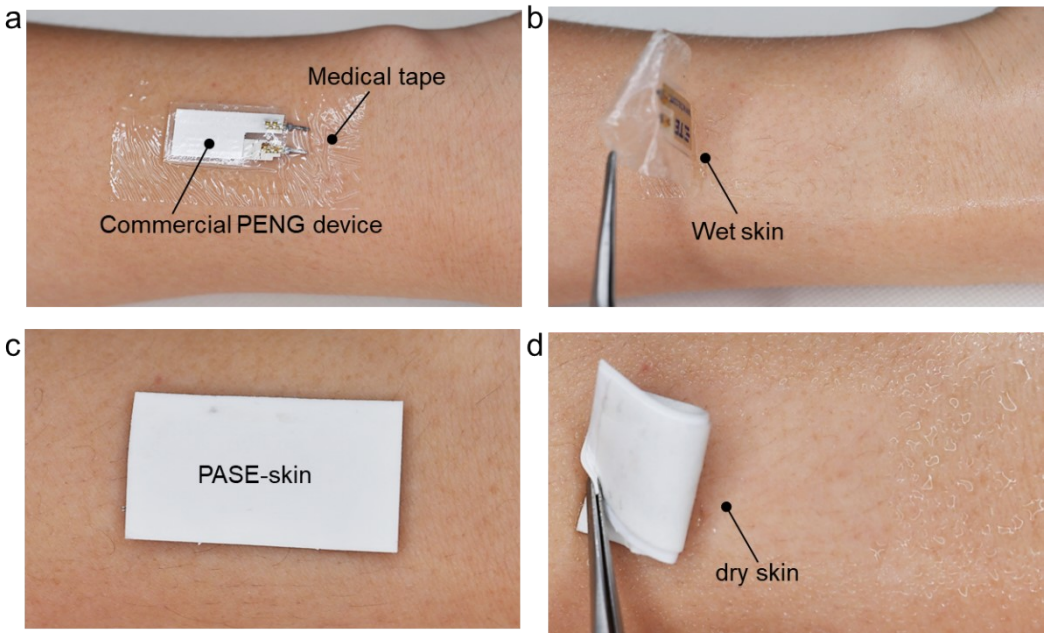

Supplementary Figure 6. Digital images of commercial PENG device attached to the human skin before (a) and after sporting (b) and PASE-skin adhered to the human skin before (c) and after sporting (d).

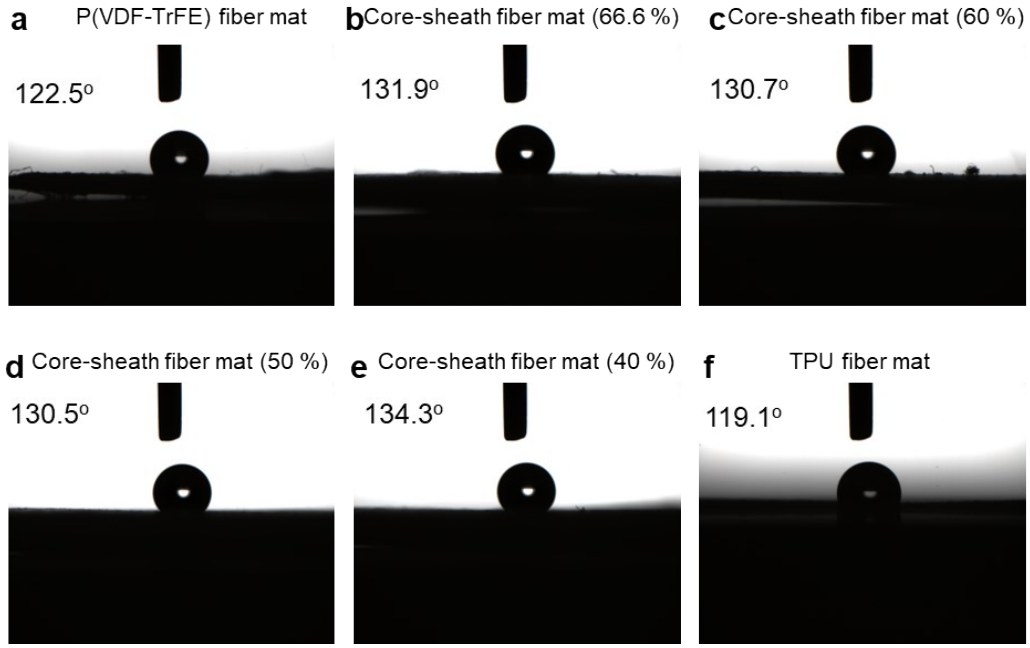

Supplementary Figure 7. Water contact angle of P(VDF-TrFE) fiber mat (**a**), TPU@P(VDF-TrFE) core-sheath fiber mat of P(VDF-TrFE) content of 66.6% (**b**), 60% (**c**), 50% (**d**), and 40% (**e**), and TPU fiber mat (**f**).

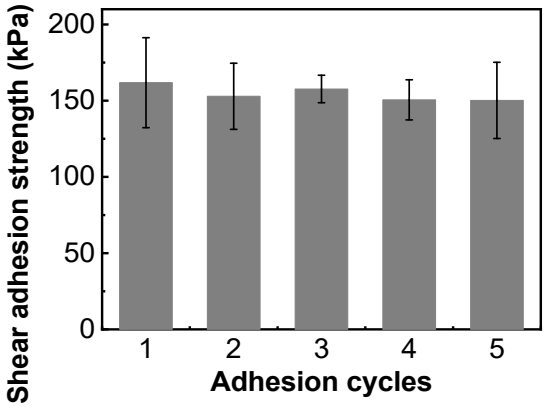

Supplementary Figure 8. Cyclic adhesion tests for the PASE-skin.

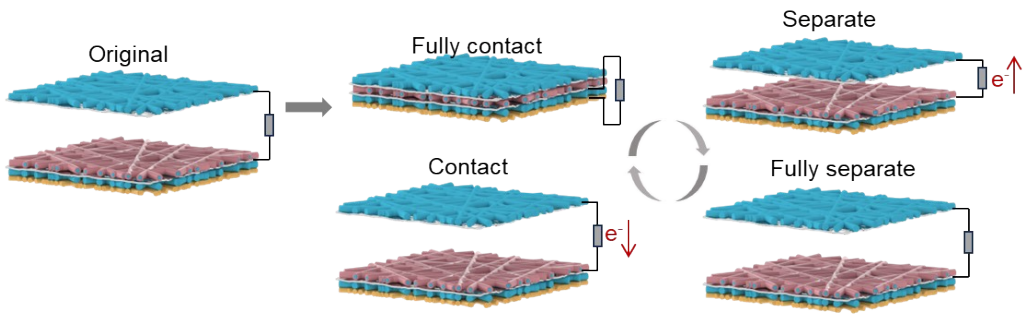

Supplementary Figure 9. Working mechanism of the PASE-skin device.

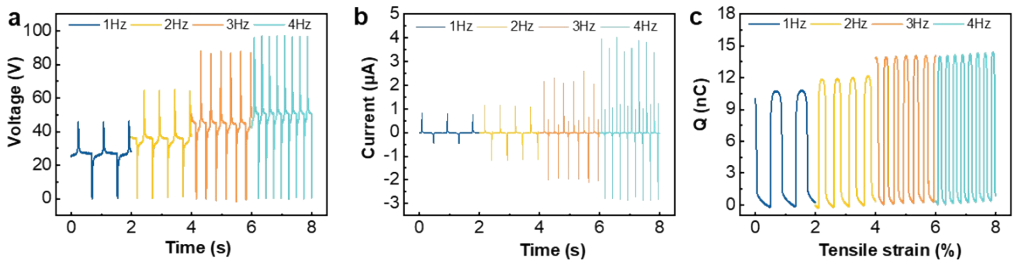

Supplementary Figure 10. a-c, Open-circuit voltage (**b**), short-circuit current (**c**) of the TPU@P(VDF-TrFE) core-sheath fiber mat (P(VDF-TrFE ratio = 40%)) with different contact-release frequencies.

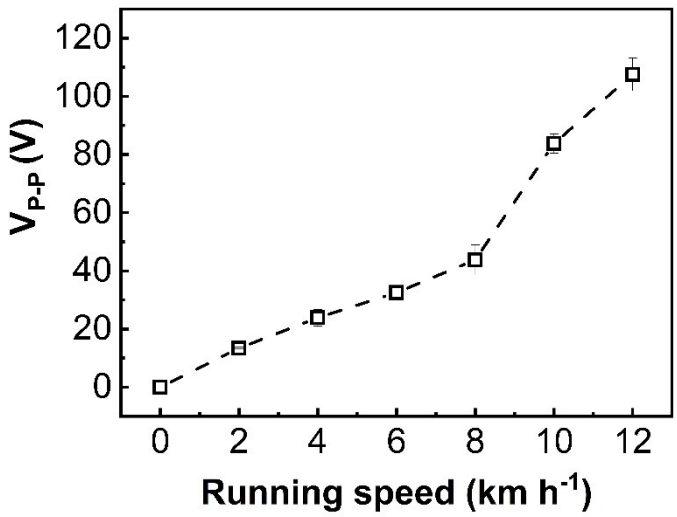

Supplementary Figure 11. The peak-to-peak voltage (Vp-p) of the PASE-skin attached to the popliteal fossa to record running speeds.

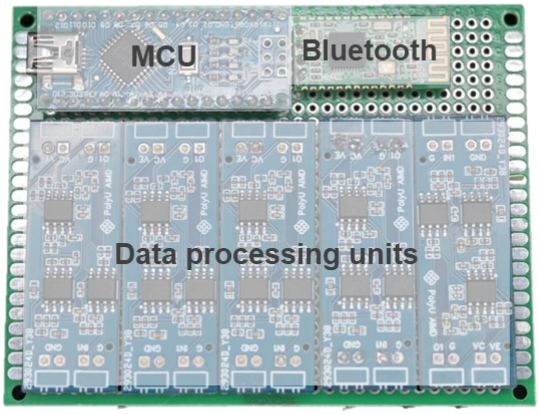

Supplementary Figure 12. Digital image of the printed circuit board (PCB) with a microprogrammed control unit, a Bluetooth, and five data processing units for amplifying, converting, and transmitting the signals from PASE-skin.

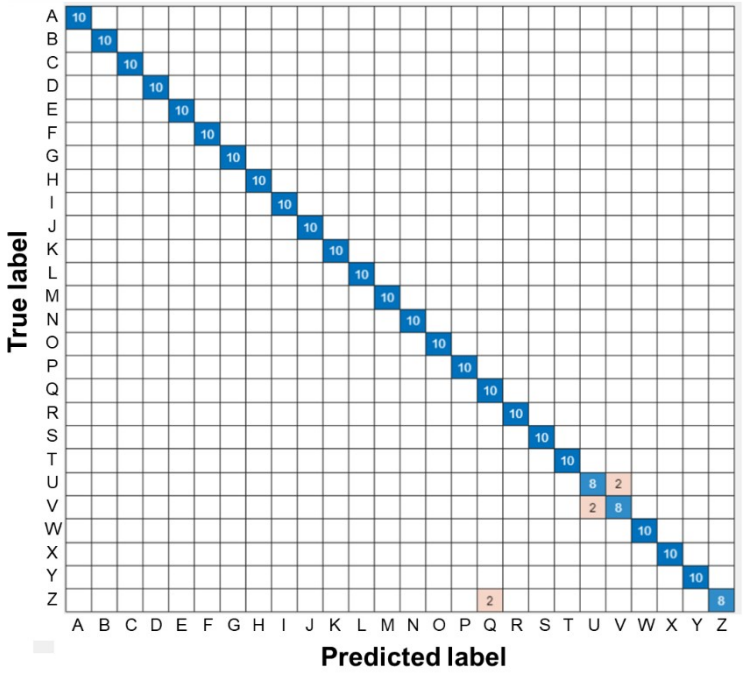

Supplementary Figure 13. Confusion matrix of the 26 types of alphabets from “A” to “Z” assisted by machine learning.

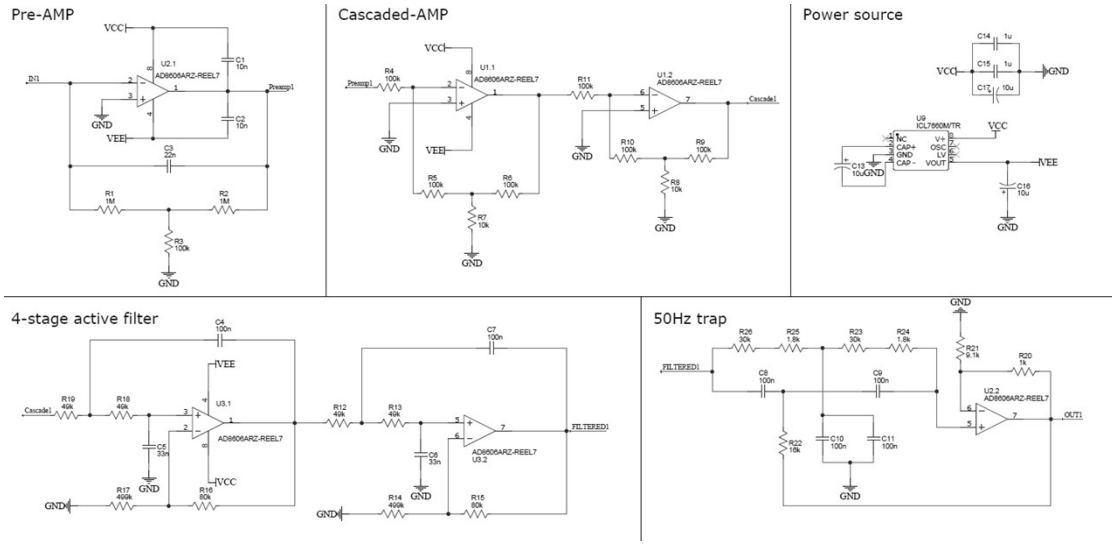

Supplementary Figure 14. Circuit diagram of signal processing unit.

Supplementary Table 1. Comparison of self-powered sensors in adhesion, permeability, stretchability properties

Materials	Permeability	Stretchability	Adhesion	Application	Ref.
Core-sheath fiber mat Liquid-metal fiber mat	**678 g m^{-2} day^{-1}**	**600%**	**147 kPa**	**Gesture recognition system**	
PLGA/PVA fiber mat	120 mm s^{-1}	300% (substrate)	/	E-skin	[1]
P(VDF-TrFE) fiber mat Conductive fabric	61.30 mm s^{-1}	/	/	E-textile	[2].
CNT/PVDF-HFP fiber mat	12 kg m^{-2} day^{-1} (38°C)	/	8 kPa	Plant sensor	[3]
P(VDF-TrFE)/PA66 fiber mat Stainless steel yarn	164 mm s^{-1} 531 kg m^{-2} day^{-1}	/	/	Self-powered E-textile	[4]
LM/SBS fiber mat/hydrogel	/	500%	0.28 N cm^{-1}	Gesture recognition system	[5]
P(VDF-TrFE) fiber mat PDMS/Au	/	30%	/	Mechanical sensor	[6]
PVDF-HFP fiber mat	Yes	/	/	E-textile	[7]
PVDF fiber mat PET/Al	/	/	/	Self-powered system	[8]
PVDF/PAN fiber mat Mxene/CNT	13.99 kg m^{-2} d^{-1}	40%	/	Health monitoring	[9]
SEBS/PVDF-HFP fiber mat Ag flakes/LM	913 g m^{-2} day^{-1}	150%	/	E-skin	[10]
Perovskite/SEBS/PVDF-HFP fiber mat	10 kg m^{-2} d^{-1},	100%	/	Energy harvesters	[11]
Fluorinated film/ aluminum foil PVDF/PVA fiber mat	/	/	16 N	Energy harvesters	[12]

Description of videos

Supplementary video 1. Demonstration of the operation of real-time gesture recognition by the PASE-skin.

References

[1] X. Peng, K. Dong, C. Ye, Y. Jiang, S. Zhai, R. Cheng, D. Liu, X. Gao, J. Wang, Z. L. Wang, *Science Advances,* 2020, **6**, eaba9624.

[2] W. Yang, W. Gong, C. Hou, Y. Su, Y. Guo, W. Zhang, Y. Li, Q. Zhang, H. Wang, *Nature Communications***, 2019**, *10*, 5541.

[3] L. Lan, J. Xiong, D. Gao, Y. Li, J. Chen, J. Lv, J. Ping, Y. Ying, P. S. Lee, *ACS Nano,* 2021, **15**, 5307-5315.

[4] X. Guan, B. Xu, M. Wu, T. Jing, Y. Yang, Y. Gao, *Nano Energy* 2021, **80**, 105549.

[5] H. Zhou, W. Huang, Z. Xiao, S. Zhang, W. Li, J. Hu, T. Feng, J. Wu, P. Zhu, Y. Mao, *Advanced Functional Materials,* 2022, **32**, 2208271.

[6] S. H. Park, H. B. Lee, S. M. Yeon, J. Park, N. K. Lee, *ACS Appl. Mater. Interfaces*, 2016, **8**, 24773-24781.

[7] Z. Zheng, X. Ma, M. Lu, H. Yin, L. Jiang, Y. Guo, *ACS Appl. Mater. Interfaces,* **2024**, *16*, 10746-10755.

[8] K. Shi, B. Sun, X. Huang, P. Jiang, *Nano Energy,* 2018, **52**, 153-162.

[9] C. Zhi, S. Shi, S. Zhang, Y. Si, J. Yang, S. Meng, B. Fei, J. Hu, *Nano-Micro Lettters,* 2023, **15**, 60.

[10] Y. Li, J. Xiong, J. Lv, J. Chen, D. Gao, X. Zhang, P. S. Lee, *Nano Energy*, 2020, **78**, 105358.

[11] F. Jiang, X. Zhou, J. Lv, J. Chen, J. Chen, H. Kongcharoen, Y. Zhang, P. S. Lee, *Advanced Materials,* 2022, **34**, e2200042.

[12] W. Du, J. Nie, Z. Ren, T. Jiang, L. Xu, S. Dong, L. Zheng, X. Chen, H. Li, *Nano Energy,* 2018, **51**, 260-269.